

# Preparation and Characterization of Unconventional Lanthanum Cerium Copurathin Films Superconductors for Development of Thermoelectric Devices

Kaltham B. Aljaloud<sup>1</sup>, Anna Kusmartsev<sup>2</sup>, Mervette El Batouti<sup>3\*</sup>

<sup>1</sup>Department of Physics, Qassim University, Saudi Arabic Kingdom

<sup>2</sup>Department of Physics, school of science, Loughborough, United Kingdom

<sup>3</sup>Chemistry Department, Faculty of Science, Alexandria University.

**\*Corresponding Author:** Mervette El Batouti, Chemistry Department, Faculty of Science, Alexandria University.

**Abstract:** Temperature dependences of thermal conductivity ( $k$ ) and electrical resistivity, for two prepared samples ( $s_1$ ,  $s_2$ ) of Lanthanum Cerium Copurate Thin:  $\text{La}_{2-x}\text{Ce}_x\text{CuO}_4$  (LCCO) with doping Ce percent ( $x \approx 0.10$ ), for ( $s_1$ ), ( $x \approx 0.12$ ) for  $s_2$  of electron-doped high temperature superconductors  $\text{La}_{2-x}\text{Ce}_x\text{CuO}_4$ . Superconductors obtained as an ultra thin film with a thickness of less than 100 nm on  $\text{SrTiO}_3$  substrate. A promising modified steady-state method was used for measurement of thermal conductivity for one optimally doped  $s_2$  and one slightly overdoped  $s_1$  at the temperature range of 3–270 K, in the absence of any applied magnetic field. The errors due to heat flow in lead wires and heat loss by radiation were minimized via fixing the heating rate of one end and the cooling rate of the other end of the test sample. Each prepared sample showed a unique thermal conductivity with a maximum at a specific critical ( $T_c$ ) temperature and an exponential dependence on temperature in the low temperature region. The distinct behavior for  $s_1$  and  $s_2$  is attributed to different doping percent ( $x$ ), and  $\text{O}_2(\text{g})$  content which altered the scattering of phonon. The temperature behavior of  $k$  for  $s_1$  is more consistent with those found in underdoped samples. However, electrical resistivity data imply that  $s_1$  is slightly overdoped. This may be explained through possible changes in  $\text{O}_2(\text{g})$  content and the possibility that  $s_1$  may actually be an underdoped sample with an increased  $\text{O}_2(\text{g})$  content. A sharp peak developed in  $k$  when superconducting transition or critical temperature ( $T_c$ ) approached. Wiedemann-Franz law was not valid over the studied temperature range, signifying the presence of strong phonon contributions to  $\kappa$  value that equals the sum of both lattice and electronic conductivity.

**Keywords:** Thin film, thermal conductivity, doping, superconductors, Superconductors, thermal conductivity, electronic conductivity, phonon.

## 1. INTRODUCTION

Unconventional and high temperature superconductors are fascinating materials in modern solid state physics and materials science and are widely used in manufacturing of wires, tapes, cables, electrical electrodes, etc. .... Moreover, these thermoelectric materials (TE) are widely used for manufacturing of transistors and microelectronics.<sup>1</sup> Superconductivity was exhibited by Hg below  $T_c$  of 4.2 K; (La-Ba-CuO) ceramics at  $\sim 30$  K; Y-Ba-O at 93 K; Bi and Tl cuprates at 125 K; Hg-based cuprates at 164 K.<sup>2</sup> A perfect superconductor elements: Pb, Ta, and Sn have zero electrical resistance and perfect diamagnetism if cooled below  $T_c$ .<sup>3</sup> Cuprates are the bases of many superconductors of different  $T_c$ : Ba-Ca-CuO;  $T_c$  120 K [3],  $\text{Ln}_{2-x}\text{Ce}_x\text{CuO}_4$  (Ln = La, Nd, Pr, Sm, or Eu) where electron-doped high- $T_c$  superconductors are less good-understood than their hole-doped counterparts.<sup>4,5</sup> Electron-doped films exhibit superconductivity extending to  $x$  below 0.10,  $(\text{Pr}, \text{La})_{2-x}\text{Ce}_x\text{CuO}_{4+\delta}$  compounds where  $T_c$  is a function of Ce-doping concentration.<sup>6</sup> However, their measured thermal conductivity was in doubt due to the errors introduced during experiment measurements.<sup>6</sup>

Many reported methods for measurement of  $k$  have challenges. Static DC absolute techniques; rapid semi-quantitative and transient method; Photoacoustic technique.<sup>7</sup> Challenges in steady-state methods, issue to the heat sink.<sup>8</sup> However Wiedemann-Franz (WF) law determine electronic thermal

conductivity  $k_c$ ; Comparative technique (standard in the series between the heater and sample);  $\omega$  technique accurately measures  $k$  and the heat capacity of a material for a simple heater geometry using diffusion equation.<sup>9</sup>

Temperature measured by thermocouple depending on Seebeck effect that is a function of the temperature difference ( $\Delta T$ ) may give a reliable measurement of  $k$ . Electrons diffuse from the hot end toward the cold end of a conductor and a potential difference developed that is directly proportional to ( $\Delta T$ ) between the heater ( $T_H$ ), and the sink ( $T_S$ ).<sup>10</sup>

$$\text{Seebeck effect, } S = \frac{\Delta V}{\Delta T} = \frac{\Delta V}{(T_H - T_S)} \quad (1)$$

$$\Delta V = (V_H - V_S)$$

Two different metals or alloy's end,  $\Delta V$  develop measure the temperature ( $T$ ) at a local position, electric current flow due to ( $\Delta T$ ).<sup>11</sup> Joining equal-length strips of two metals at two ends making a loop, where one end of two junctions was dipped in a source of boiling water and the other end in cold sink. Size of electric current flows through loop directly related to  $\Delta T$ . At low temperature, type E-thermocouple was determined to measure the temperature at two different locations on thin film.<sup>12</sup> Calibration Tables are used to convert thermal electromotive force (e.m.f) of a thermocouple to temperature, *via* differential reference method.<sup>13</sup>

## 2. EXPERIMENTAL

In this work, thermal conductivity measurements were conducted on a copper (Cu) sample and the prepared samples of LCCO superconductors using a thermocouple probe of two metal alloys under optical microscopic investigation. The potential difference,  $\Delta V$  developed and electric current flow due to  $\Delta T$  between the two metal ends. A sensitive E-type thermocouple wire probes (chromel (90% Ni, 10% Cu) + constantan (55% Cu, 45% Ni)) was used to monitor voltage at low temperature. To optimize the experimental condition, chromel, constantan wires of thermocouple probes were of different diameters, Table (1), cut into equal parts, glued onto the test sample at a particular location using silver (Ag)-loaded epoxy adhesive and hardener. The two wires twisted together, glued by Ag epoxy to form thermocouple forming wire probes. The Evo-stick two-parts, rapid adhesive glue have good  $k$  to ensure that the thermocouple will be in thermal equilibrium with sample, and it is thermally stable through the measurement cycling. An insulated copper wire was used as external wiring connections.

**Table 1.** Wires materials with various diameters.

| Material             | Diameter (d)     |
|----------------------|------------------|
| Chromel (Ni/Cr)      | 0.025 mm         |
| Constantan (Ni/Cu)   | 0.025 mm         |
| Cu (insulated)       | 0.125 mm         |
| Thick Cu (insulated) | $\approx 1.0$ mm |

Insulated thin Cu wires ( $d \approx 0.125$  mm) was connected directly to the sample. The thick Cu wires ( $d \approx 1.0$  mm) connected the electrical inputs (nanovoltmeter, current source, lock-in amplifier). Two types of wires were used because samples are very small ( $\approx 5$  mm). The insulation was removed from Cu wire ends, and the exposed end of Cu-wires were coated with a thin layer of suitable solder: 40% lead (Pb) plus 60% tin (Sn) at soldering temperature  $\approx 300^\circ\text{C}$ . This tinning protected Cu from air oxidation and improved soldering contact. The thermal conductivity of a copper sample was tested by taking high thermally conductive Cu foil,  $k_{Cu} = 400 \text{ W/(K.m)}$  used to check the validity of experimental method.<sup>14</sup> Test, measurement set up, is shown in Table 2.

**Table 2.** Dimensions of copper foil reference test sample.

| Dimensions       | Cu   | Error | %error |
|------------------|------|-------|--------|
| Length l (mm)    | 3.0  | 0.1   | 3      |
| Width w (mm)     | 3.0  | 0.1   | 3      |
| Thickness d (mm) | 0.30 | 0.05  | 16     |

Modification of the steady state method for measuring  $k$  was carried as follows: a Vera board having of vertical Cu conducting tracks, is used (Figure 1). The sample was connected on one end of the board and a thick external Cu wire was connected to the other end and was soldered to BNC connectors, number 3 was attached to the electrical inputs of devices (nanovoltmeter, current source,...). One sample end was glued to the “cold sink” (a simple brass post (Figure 1-number 4) using quickly dried and mechanically strong GE varnish glue. A heater (a chip resistor of  $R=100$  ohm (with knowing power,  $P = RI^2$ ) was attached to the other sample end (Figure 1- number 2). The  $\Delta T$  between the heater and the cold sink was established across Cu foil as a test sample and measured  $T_{hot}$ , and  $T_{cold}$  using the thermocouple junctions attached at two positions.

$$k_{Cu} = P \times \frac{l}{[(w \times d) \Delta T]} = \frac{l}{[(w \times d)(T_{hot} - T_{cold})]} = (1/378) \times (3/(3 \times 0.3)) \times 10^3 = 8.8 \text{ (W/K.m)} \quad (3)$$

The obtained values of  $k_{Cu}$  were compared to the known value:  $k_{Cu}=400 \text{ W/(K.m)}$ . It is likely that only a part of the heater power was transmitted through the sample and only 2.2% of heater power was going into Cu foil. During measurement of  $k$  of the prepared LCCO thin film samples, the error sources attributed aerated conditions air and the heat transfer by convection contribution to the heat flow and the purity of the tested Cu foil is high to avoid biasing of the results were minimized.

Connections of Vera board and wires were made through solder joints (Figure 1- number 3) at  $300^\circ\text{C}$ . All connection points were tested for electrical continuity using a voltmeter. Thermal conductivity of LCCO films carried out using thermocouples of the two metal alloys chromel and Constantine glued at two specific locations on the sample. Measuring  $T_{hot}$ ,  $T_{cold}$  of the heater connected at one sample end and the heat sink connected at the opposite end, The geometric dimensions (width,  $w$ ) of the substrate plus the film were recorded. The film thickness  $t$ , the distance between the two thermocouple junctions were obtained.

In this study, a linear  $\Delta T$  is assumed which is a valid approximation for small distances ( $\approx 10\text{mm}$ ) to include the physical effects of the heater connections, interfaces and the power loss due to the cables or the connections is minimized.<sup>15-22</sup>

In our study, It is thought that the error source of estimation of sample's geometry and the quality of Cu foil surface is controlled, Table(2). However, the total error due to the geometric factor  $\approx 5\%$  did between the measured ( $k_{Cu}$ ) and the accepted value of  $k_{Cu}=400 \text{ (W/K.m)}$  for Cu. The error source of Cu foil surface quality is minimized and controlled by working the experimental measurements under deaerated conditions.

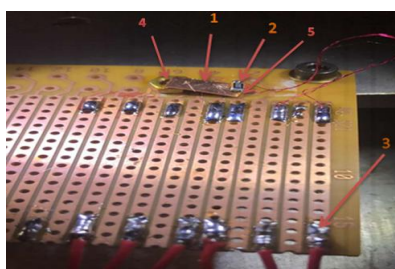


Figure 1. Soldering station with a circuit board.

Where: 1. thermocouples; 2. heater; 3. solder points.; 4. cold sink; 5. Cu foil.

### 3. RESULTS AND DISCUSSION

The voltage developed across the thermocouple was monitored with time, and represented in Figure 2 where:  $\Delta V = V_{hot} - V_{cold}$  was determined.

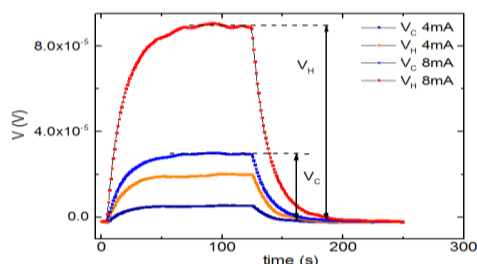


Figure 2. Two heater current values induce different voltages  $V_H$  and  $V_C$ .

A current pulse applied to the small sample heater and current response with time on thermocouple measured. Thermocouple voltage in an ON and OFF state of heater measured. A comparison between steady-state (time-independent voltage, DC) between ON and OFF heater state, determine thermocouple voltage:  $V = V_{ON} - V_{OFF}$  at different currents density: 4mA, and 8mA. The thermal voltage related to  $T_H$  and  $T_C$  at 8mA, higher heater power ( $P = I^2R$  and large thermal voltages (red and blue points, Figure 3). Measured voltages for  $I=4mA$  is much lower. To generated voltage in thermocouple reflecting the potential difference both cold  $V_C$ , hot  $V_H$ . In Figure 3,  $\Delta T$  plotted against thermopower ( $P$ ) showing the direct proportionality between the electrical power ( $P$ ), and  $\Delta T$  in accordance with Seebeck effect.

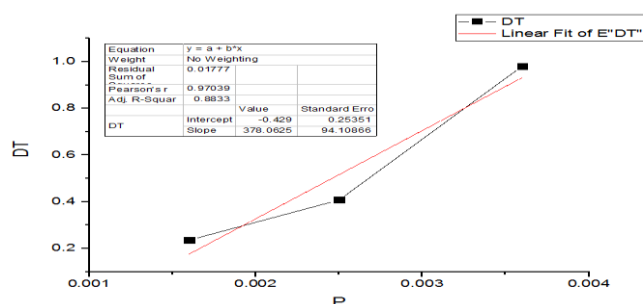


Figure3. Difference  $\Delta T$  against thermopower  $P$ .

The temperature increased linearly with increasing thermopower ( $P$ ). The red line represents a fitting of curve using a linear equation:

$$\Delta T = a * P + b \tag{4}$$

The fit is moderately good with  $R^2 = 0.8833$ . Coefficient  $a = 378$  (K/W), and these parameters were used to calculate  $k$ . The validity of equation (4) in our study of LCCO thin film indicated that the modified thermal setup used for measuring  $k$  of the samples in this study is valid and acceptable. Figure 4 clarified that as the electric power ( $P$ ) of the heater increased, as the temperature difference ( $T_{hot} - T_{cold}$ ) was increased.

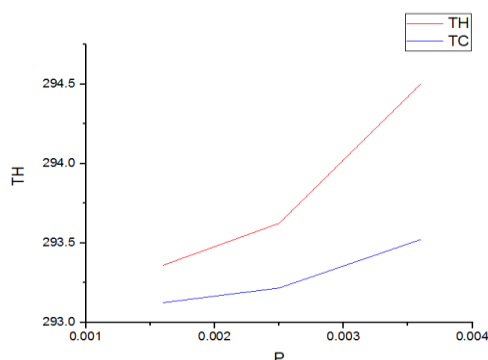


Figure3. Temperature of thermocouple  $T_H$ , and  $T_C$  against heater power  $P$ .

Figure4, showed two curves representing the temperature of thermocouple hot:  $T_{hot}$ ,  $T_{cold}$  plotted against power ( $P$ ). A significantly higher ( $T_H$ ,  $\Delta T = T_{hot} - T_{cold}$ ) was observed.

### 3.1. Preparation of L-Platform and Electrical Connections for Measurement of $K$ for LCCO.

The two prepared (LCCO) thin films with different Ce-doping ( $x$ ) were described in Table 3 corresponding to:  $5K < T_C < 27K$  measured through the thermal transport.

Table3. Sample description.

| Samples | Chemical formula                         |
|---------|--|
| $S_1$   | $La_{2-x}Ce_xCuO_4$ ( $x \approx 0.12$ ) |
| $S_2$   | $La_{2-x}Ce_xCuO_4$ ( $x \approx 0.10$ ) |

Sample thin geometry is shown in Table 4 indicated that both the samples are air stable and stored outside a desiccator.

**Table4.** Samples s1 and s2 geometry dimensions:

| LCCO      | S1    | S2    |
|-----------|-------|-------|
| Width     | 3mm   | 3mm   |
| Length    | 1.8mm | 2.4mm |
| Thickness | 200nm | 200nm |
| Error     | 0.1   | 0.1   |

### 3.2. Making Electrical Connections to L-Shaped Platform

The experiment was started with a blank L-platform. Plastic tracks attached to Ni pads to the L-shaped platform. Pads soldered to and used as connection points for the wires from the sample and cryostat connector. Plastic tracks attached to L-platform using a STYCAST resin- STYCAST 2850 FT. Resin STYCAST 2850 FT and CATALYST 23 LV are mixed in right proportions 7.5% weight using. Small amounts of powder  $Al_2O_3$  catalyst was added to STYCAST 2850 FT until a viscous mixture to improve thermal conductivity and mechanical strength of TYCAST. Once mixed, resin was used to attach plastic tracks – in two rectangular, thin strips to L-platform – at either edge (Figure 5-number 1). Thin insulated Cu wires ( $d=0.125mm$ ) was cut in equal sized segments of 7-8cm, endstinned, twisted into pairs to improve soldering contacts and reduce induction noise. One end of a twisted wire pair soldered onto Ni-pads on the L-platform, and other end soldered to a 12-pin connector from which 8 connections used. Pins 1 and 2 were for hot thermocouple  $T_H^+$  and  $T_H^-$  respectively. Pins 5, 6) were for cold thermocouple  $T_C^+$  and  $T_C^-$  respectively. Pins 11 and 12 deliver the current through the heater, pins 9 and 10 were used to perform a four points measurement of heater resistance  $R_s$  as shown in Figure (5).

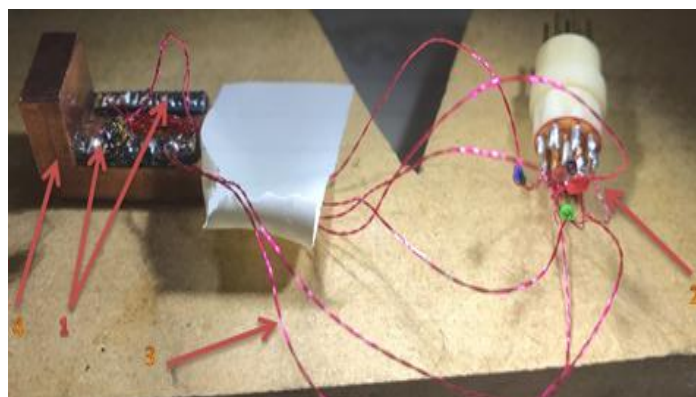


**Figure5.** L-platform with electrical connections. 1 STYCAST resin connecting tracks; 2 – 12-pin connector attaching to cryostat; 3- Cu wire; 4 L-platform.

Sample attached with L-shaped platform using a STYCAST resin - STYCAST 1266 (part A), part B (ethyleneoxy) bis (propylamine) were mixed in right proportions 28wt% of part, and small amounts  $Al_2O_3$  powder was added to STYCAST until a viscous mixture obtained, Mixture was put in (Hotbox Oven With Fan at  $70^\circ C$  for 5 min. to be viscous and to minimize out gassing in desiccator. A suitable mixture obtained and was attached to the sample in the platform by glue (Figure 6).

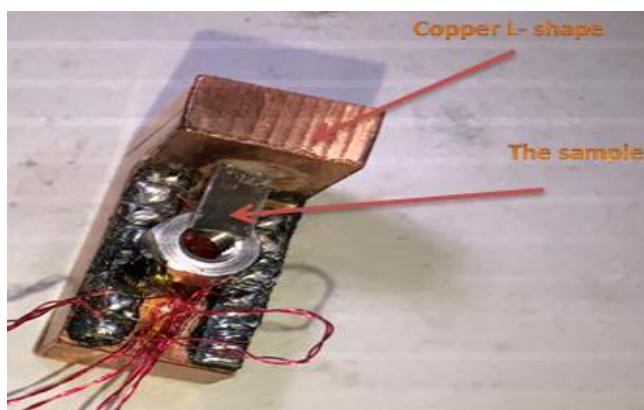


**Figure6.** Sample attached with L-shaped platform.

Sample attached to the heater tousing STYCAST 1266resin prepared by the same process of the last stage. The sample was put in a desiccator, because LCCO is air sensitive. (Figure 7)

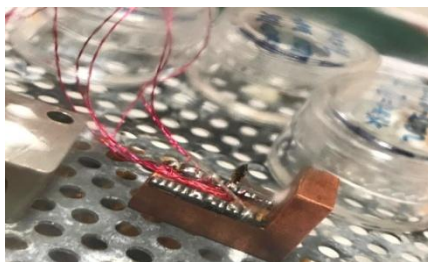


Figure7. Sample attached with small heater.

So, two thermocouples used during  $k$  measurement, (Figure 8).

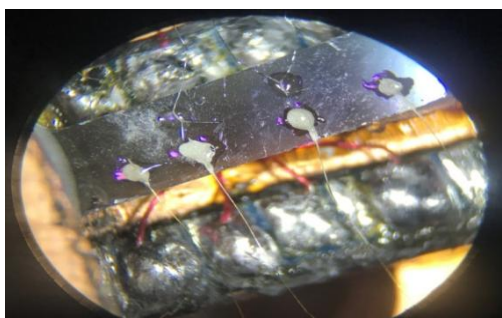


Figure8. Thermocouples under microscopic.

### 3.3. Cryogenic Experiments

LowCryogenic temperatures 3 -295K used to study LCCO achieved using a Gifford McMahon closed cycle cryostat under an ultra-high vacuum of  $\sim 10^{-5}$  mbar using a combination of a roughing and a turbo pumps to minimize heat convection through the surrounding medium .<sup>18, 19-22</sup> Low temperatures 3K obtained using a Gifford McMahon closed cycle cryostat system consists of 2 stages, measurements conducted on 2<sup>nd</sup> stage [16]. The sample is attached electrical connectors Au leads to sample and gluing L-shaped platform to cryostat platform, Figures 9 and 10 showed the connection of the sample with cryostat.

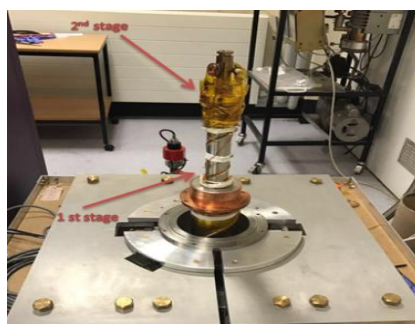


Figure9. Different stages in the cryostat system.

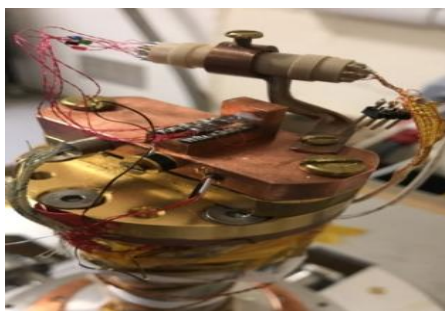


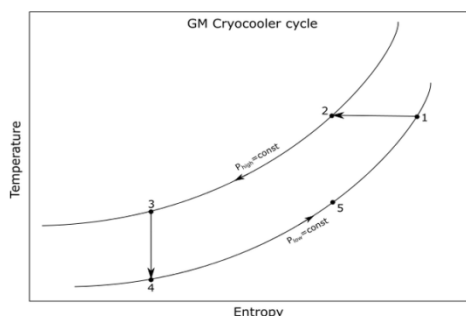
Fig10. Sample with cryostat.

Table 5 showed the complete description of the cooling conditions.

**Table 5.** Temperature and cooling power for cold sink component.

| Cold head component   | Temperature (K) | Cooling Power (W) |
|-----------------------|-----------------|-------------------|
| 1 <sup>st</sup> stage | 40K             | ~50W at 40K       |
| 2 <sup>nd</sup> stage | 3K              | ~1.0W at 4K       |
| Exterior of cryostat  | 295K            | 0                 |

Gifford-McMahon (GM) refrigerator in cryostation system during a cycle was used. Figure 11 showed a simplified description of this technicality [23]. A temperature versus entropy diagram of cycle. Figure 11 illustrated the cooling cycle process of the system components. (from top left-right, bottom left-right) [25].



**Figure 12.** Temperature versus Entropy diagram in Gifford-McMahon cooling cycle [25].

By motor displacer driven, at any period during the cycle when displace either at the chamber bottom or to because of forced motor. Rotating valve sometimes used in description of GM cooler replaced by a high pressure and low pressure, And closure of a valve, or closure of a given port can indicate by cross on port. As a separate chamber regenerator in parallel with chamber holding Displacer (because regenerator embedded within displacer). Sample area can be thought of as a heat exchanger in thermal contact directly with lower chamber under the displacer.

Figure (11) showed that at point 1-2: at bottom with displacer, constant temperature, high pressure inlet opened and upper chamber pressurized; at points 2-3 and low pressure exhaust port was closed, displacer moved to top forcing move gas out from the top chamber out of regenerator to the lower chamber at constant pressure for gas cooling due to operations 4-5-1 which already cooled regenerator. At points 3-4: at the top with displacer, low pressure exhaust port opened to allow gas in the lower chamber to cool and expand. Expansion for displaced some gas out during exhaust port for doing some work. In GM cycle for cooling gas, direct thermal contact drive heat out of sample space points 4-5-1: cooled stage, Displacer moving down with low temperature gas forced out of the chamber. Cooling regenerator, at low pressure port, gas leaves at a nearly ambient temperature.<sup>24-26</sup>

Thermal conductivity of two (LCCO) films dependence on temperature in range 3-270K is represented. The raw data obtained during warmup, starting from 3K. GM closed cycle refrigeration (CCR) crystal was used. A Lab. view program automated measurement was carried out. Temperature sweeping rate and step improved the measurements accuracy. At low temperatures, temperature step 0.2K was used to investigate the transition between superconducting and normal states. At high temperatures, 1.0 K temperature step was used<sup>17</sup>. The data were analyzed through a custom written Python script. Measurement parameters of s1 and s2 were summarized in Table 6.

**Table 6.** Measurement parameters.

| Temperature range (K) | Temperature step (K) | Sweep rate (K/min) |
|-----------------------|----------------------|--------------------|
| 3 -60                 | 0.2                  | 0.2                |
| ~60 – 160             | 0.5                  | 0.3                |
| ~160 – 270            | 1.0                  | 0.5                |

The electrical transport in Ce-doped (LCCO) samples was determined and the resistivity measurements yield  $T_{C-S1} = 23.5$  K,  $T_{C-S2} = 26.5$  K for s1 and s2 respectively. Transition estimated at

50% value of normal state resistivity. Doping percent of Ce estimated by comparing the experimental  $T_c$  to the literature.<sup>26</sup> It was found that s1 is optimally doped sample with  $x=0.1$  and s2 is a slightly overdoped sample with  $x=0.12$ .

Thermal conductivity of s1 and s2 showed in Figure (12) is in good agreement with the published results.<sup>26</sup> A peak appeared in the low temperature region. While  $k$  is almost temperature independent at high temperatures, particularly for s1. Temperature behavior in  $k$  for s1 is more consistent with those found in underdoped samples [26], Figure(12). However, resistivity data imply that s1 is slightly overdoped. This may be explained through possible changes in  $O_{2(g)}$  content as increasing  $O_{2(g)}$  content increased the low temperature peak in  $k$ .<sup>26</sup> Figure (12), It is possible that s1 may actually be an underdoped sample with increased  $O_{2(g)}$  content  $La_{2-x}Ce_xCuO_4$ . The (LCCO) films s1 and s2 have  $T_{C-s1}=23.5$  K and  $T_{C-s2}=26.5$  K. Figures 12, 13 represented the measurement of  $k$  dependent temperature for sample s1 and s2. The nominal composition from resistivity measurement is close to optimal approximately,  $x=0.12$ ,  $x=0.10$  for s1, and s2 respectively. The peak of s1 is much bigger than that of s2. Thermal conductivity of sample 1 is almost temperature dependent above 200 K. However, the behavior of s2 is quite different.

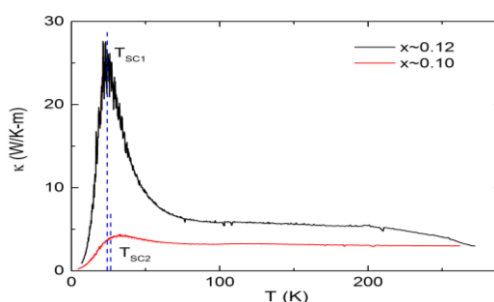


Fig12. Thermal conductivity S1 and S2 as a function of temperature of.

$T_{SC1}$  and  $T_{SC2}$  referred to the superconducting temperatures obtained from electrical transport. A sharp peak in  $k$  indicates an approach to the superconducting state, may be important for its mechanism and origin.

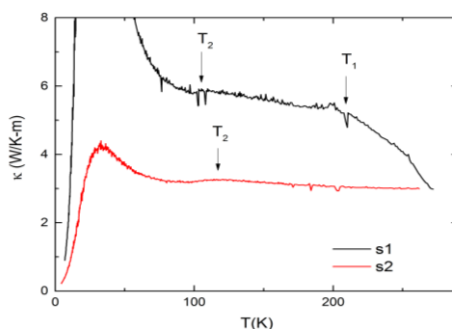


Figure13. Thermal conductivity measurement of S1 and S2 as a function of temperature.

$T_1$  marks a significant change in temperature behavior of  $k$  for s1 then the behavior becomes almost temperature independent. Above  $T_1$ ,  $k$  rapidly decreases.  $T_2$  indicates the position of a slight peak in thermal conductivity ( $k$ ) for s1 and s2 around 100 K.

From resistivity and the high-temperature thermopower results, s1 looks to be slightly overdoped, Ce-doping  $x \approx 0.12$ . However, ( $k$ ) values results not agree with this simple picture. For s1 thermal conductivity is significantly higher at lower temperatures than for s2. Peak around  $T \sim T_C$  is much more pronounced in s1 compared to s2 (Figure 13). At  $T > 150$  K,  $k$  in s1 has a sharp change in slope – marked at  $T_1$  (Figure 6.2). These features are all consistent with  $k$  temperature dependence found in underdoped samples (Figure 14).<sup>26</sup> Such underdoped samples did not show superconductivity. Around 100 K a broad shoulder-like anomaly indicated at  $T_2$  becomes obvious both for s1 and s2 (Figure 12). This anomaly does not show strong doping dependence in the Ce-doping range studied.

It was reported that, doping dependence ( $k$ ) of  $Pr_{1.3x}La_{0.7}Ce_xCuO_4$  looked to be in a good agreement to s1.<sup>26</sup> As Ce-doping increased both in-plane  $k_{ab}$  and out-of-plane  $k_c$  thermal conductivities



decreased and the peak around  $T_C$  becomes less pronounced. This finding may be attributed to the oxygen content in s1 that explained the observed discrepancy in comparison, influence of  $O_2$  on  $Pr_{1.3-x}La_{0.7}Ce_xCuO_4$ .<sup>26</sup> The out-of-plane  $k_c$ , low temperature peak is less pronounced when more  $O_2$  added. In-plane  $k$ , no such significant changes observed. For s1, oxygen content different from s2. If composition for s1:  $La_{2-x}Ce_xCuO_{4+}$  explain lower nominal doping  $x$ , and high superconducting  $T_C=23.4K$ .

The low temperature behavior of  $k$  was studied using the thermal exponential model:

$$\kappa = AT^n \tag{5}$$

The data of thermal conductivity of s1 and s2 were fitted to determine the best value of the exponent (n). The obtained results are illustrated in Figure(14).

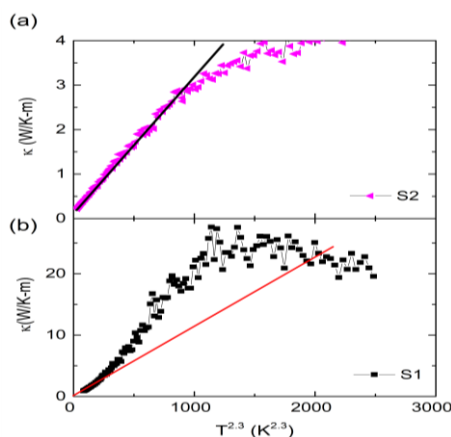


**Figure14.** Low temperature dependence of  $k$ : (a) optimally doped LCCO s2 ( $x = 0.10$ ), (b) slightly overdoped s1 ( $x = 0.12$ ).

Figure 15 showed that thermal conductivity at low temperature ( $k$ ) for s2 (optimal doping) showed a good  $\approx T^{2.3}$  temperature dependence and thermal exponents was valid up to 14-16K. While the values  $k$  for s1 (nominally slightly overdoped) did not follow this  $T^{2.3}$  behavior. This confirms that the doping percent, significantly affects the thermal transport of s1, and s2.

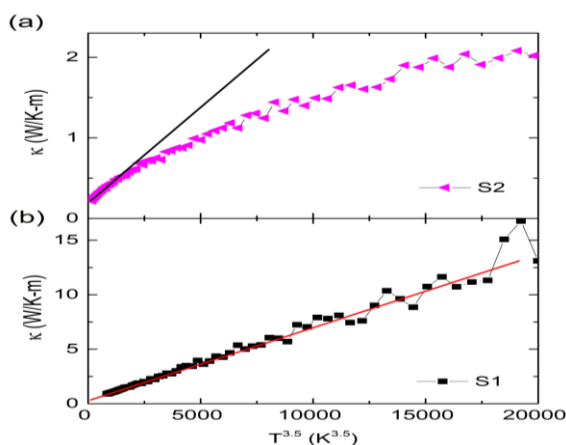


**Figure15.** An alternative model for temperature dependence of  $k$ : (a) optimally doped s2 ( $x = 0.10$ ) (b) slightly overdoped s1 with doping  $x = 0.12$ .

$k$  for s1 shows a good  $\sim T^{3.5}$  temperature dependence. While  $k$  for s2 not follow the  $T^{3.5}$  behavior.

The different behavior of  $k$  between s1 and s2 is substantial. It may be that a simple change in Ce-doping not cause this difference in behavior. This low-temperature analysis adds further confirmation that  $O_{2(g)}$  content should be considered. The electronic  $k$  calculated according to Wiederman-Franz law:

$$\kappa_e = \frac{L_0 T}{\rho} \tag{6}$$

Where  $L_0 = 2.44 \times 10^{-8} \text{ W}\Omega\text{K}^{-2}$ . Calculated electronic resistivity,  $\kappa_e$  for s1 at 270K

$$\rho_{s1}(270\text{K}) = 1.736 \times 10^{-5} \Omega\text{-m.}$$

$$k_e(270\text{K}) = L_0 \times 270 / \rho = 2.44 \times 10^{-8} \times 270 / 1.736 \times 10^{-5} = 0.379 \text{ W/K-m,}$$

$$\text{Total } k_{s1} \text{ at 270K: } \kappa \sim 3.0 \text{ W}\text{K}^{-1}\text{m}^{-1}$$

Electronic thermal conductivity,  $\kappa_e$  is much less than total  $k$ ,  $\kappa_e \ll \kappa$ .

A similar trend was observed in s2 resistivity is  $\rho_{s1}(270\text{K}) = 2.05661 \times 10^{-5} \Omega\text{-m}$ . Same calculation was provided for  $\kappa_{e s2}$ :

$$k_e(270\text{K}) = L_0 \times 270 / \rho = 2.44 \times 10^{-8} \times 270 / 2.05661 \times 10^{-5} = 0.320 \text{ W/K-m}$$

$$\text{Total } k_{s2} \text{ at 270K } \kappa \sim 3.0 \text{ W}\text{K}^{-1}\text{m}^{-1}$$

For optimally doped s<sub>2</sub>, much less than total  $\kappa_{e s2} \ll \kappa$  implying that lattice and phonons contribute the thermal transport in thin film samples LCCO. Similar behavior found in other prviously prepared cuprates superconductors.<sup>25</sup> Table 7 showed the application Wiedermann-Franz ratio

k of S1, S2 using Wiedermann-Franz ratio.

**Table 7.** k of S1, S2 using Wiedermann-Franz ratio.

| Sample | keW/K-m) | Electrical resistivity, $\Omega\text{-m}$ ) | Wiedermann-Franz ratio at 270K | T <sub>C</sub> (K) |
|--------|----------|---|--------------------------------|--------------------|
| S1     | 0.379    | $1.736 \times 10^{-5}$                      | 7.9                            | 23.5               |
| S2     | 0.320    | $2.05661 \times 10^{-5}$                    | 9.4                            | 26.5               |

High Wiedermann Franz ratio  $\gg 1$  indicated strong photonic processes in LCCO at optimally doping (s2) and slightly over doped (s1). A similar behavior in the temperature dependence of k in single crystal  $\text{La}_{1.602x}\text{Nd}_{0.40}\text{Sr}_x\text{CuO}_4$  ( $x = 50.12, 0.15, 0.20$ ) (a) in a-b plane, along c-axis. Lower part of (a) shows electronic contribution  $k_e$  in the ab-plane from electrical data *via* Wiedermann-Franz law [15] where hole-doped cuprate superconductors:  $\text{La}_{1.602x}\text{Nd}_{0.40}\text{Sr}_x\text{CuO}_4$  in over-doped range. The values of  $k_e$  calculated from Wiedermann Franz Law. The large discrepancy between  $k_e$  and total demonstrate that W-F law may not be valid over the entire temperature regime. However, W-F regime being approached with higher doping.

#### 4. CONCLUSION

Thermal conductivity (k) studied for one optimally doped (s2) and one slightly over doped (s1) sample (LCCO) films in the temperature range 3-270K. A sharp peak was developed in thermal conductivity as superconducting transition temperature T<sub>C</sub> is approached. Wiederman-Franz law was not valid over the studied temperature range, signifying the presence of strong phonon contributions to the thermal conductivity. A peak in thermal conductivity is obtained at the low temperature region and there is an exponential decrease of k at the high temperature region. Wiederman-Franz law was not valid over the studied temperature range, signifying the presence of strong phonon contributions to the thermal conductivity. The values of  $k_e$  are much less than total thermal conductivity  $\kappa_e \ll \kappa$  indicating that the lattice and phonons are the controlling factors for thermal transport in (LCCO) rather than electrons.

#### REFERENCES

- [1] Vandersande, I.W., Ewell, R., Fleurial, J.P. and Lyon, H.B., California Institute of Technology, 1998. Cooling device featuring thermoelectric and diamond materials for temperature control of heat-dissipating devices. U.S. Patent 5,712,448.
- [2] Krockenberger, Y., 2006. Epitaxial thin film growth and properties of unconventional oxide superconductors. Cuprates and cobaltates.
- [3] Bennemann, K.H. and Ketterson, J.B. eds., 2008. Superconductivity: Volume 1: Conventional and Unconventional Superconductors Volume 2: Novel Superconductors. Springer Science & Business Media.
- [4] Tranquada, J.M., Heald, S.M., Moodenbaugh, A.R., Liang, G. and Croft, M., 1989. Nature of the charge carriers in electron-doped copper oxide superconductors. Nature, 337(6209), p.720.

- [5] Sawa, A., Kawasaki, M., Takagi, H. and Tokura, Y., 2002. Electron-doped superconductor  $\text{La}_{2-x}\text{Ce}_x\text{CuO}_4$ : Preparation of thin films and modified doping range for superconductivity. *Physical Review B*, 66(1), p.014531.
- [6] Butch, N.P., Jin, K., Kirshenbaum, K., Greene, R.L. and Paglione, J., 2012. Quantum critical scaling at the edge of Fermi liquid stability in a cuprate superconductor. *Proceedings of the National Academy of Sciences*, 109(22), pp.8440-8444.
- [7] Rowe, D.M. ed., 2005. *Thermoelectrics handbook: macro to nano*. CRC press
- [8] Kundert, K.S., White, J.K. and Sangiovanni-Vincentelli, A.L., 2013. *Steady-state methods for simulating analog and microwave circuits (Vol. 94)*. Springer Science & Business Media.
- [9] Cahill, D.G., 1990. Thermal conductivity measurement from 30 to 750 K: the  $3\omega$  method. *Review of scientific instruments*, 61(2), pp.802-808.
- [10] Van Herwaarden, A.W. and Sarro, P.M., 1986. Thermal sensors based on the Seebeck effect. *Sensors and Actuators*, 10(3-4), pp.321-346.
- [11] Getting, I.C. and Kennedy, G.C., 1970. Effect of Pressure on the emf of Chromel- Alumel and Platinum- Platinum 10% Rhodium Thermocouples. *Journal of Applied Physics*, 41(11), pp.4552-4562.
- [12] Pollock, D., 2017. *Thermocouples: theory and properties*. Routledge.
- [13] Michalski, L., Eckersdorf, K., Kucharski, J. and McGhee, J., 2001. *Front Matter and Index (pp. i-xv)*. John Wiley & Sons, Ltd.
- [14] Nath, P. and Chopra, K.L., 1974. Thermal conductivity of copper films. *Thin Solid Films*, 20(1), pp.53-62.
- [15] Avery, A. D., Mason, S. J., Bassett, D., Wesenberg, D., & Zink, B. L. (2015). Thermal and electrical conductivity of approximately 100-nm permalloy, Ni, Co, Al, and Cu films and examination of the Wiedemann-Franz Law. *Physical Review B*, 92(21), 214410.
- [16] Pope, A. L., Zawilski, B., & Tritt, T. M. (2001). Description of removable sample
- [17] Cahill, D. G., Katiyar, M., & Abelson, J. R. (1994). Thermal conductivity of a-Si: H thin films. *Physical review B*, 50(9), 6077.
- [18] Cahill, D. G., Fischer, H. E., Klitsner, T., Swartz, E. T., & Pohl, R. O. (1989). Thermal conductivity of thin films: Measurements and understanding. *Journal of Vacuum Science & Technology A: Vacuum, Surfaces, and Films*, 7(3), 1259-1266.
- [19] Schumann, J., Kleint, C. A., Vinzelberg, H., Thomas, J., Hecker, M., Nurnus, J., Boettner, H., Lambrecht, A., Kunzel, C., and Voelklien, F., *Proceedings of 2nd International Conference on Thermoelectrics, La Grand-Motte*, p. 677, 2003.
- [20] Venkatasubramanian, R., Siivola, E., Colpitts, T., & O'quinn, B. (2001). Thin-film thermo-electric devices with high room-temperature figures of merit. *Nature*, 413(6856), 597-602.
- [21] Lee, S. M., Cahill, D. G., & Venkatasubramanian, R. (1997). Thermal conductivity of Si-Gesuperlattices. *Applied physics letters*, 70(22), 2957-2959.
- [22] Kasap, S. (2001), *Thermoelectric effects in metals: thermocouples*. Canada: Department of Electrical Engineering University of Saskatchewan.
- [23] <http://resources.montanainstruments.com/help/understanding-the-gifford-mcmahon-cryo-cooler-cycle>
- [24] Sun, X. F., Kurita, Y., Suzuki, T., Komiya, S., & Ando, Y. (2004). Thermal Conductivity of  $\text{Pr}_{1.3-x}\text{Ce}_x\text{CuO}_4$ . Single Crystals and Signatures of Stripes in an Electron-Doped Cuprate. *Physical review letters*, 92(4), 047001.
- [25] Mori, K., Tanaka, A., Nishimura, K., Isikawa, Y., Sakurai, J., Matsukawa, M., & Noto, K. (1994). Thermal conductivity and electrical resistivity of the T' phase and the T phase in 2-1-4 oxide superconductors. *Journal of superconductivity*, 7(5), 813-817.
- [26] Yan, J. Q., Zhou, J. S., & Goodenough, J. B. (2003). Thermal conductivity in the stripe-ordered phase of cuprates and nickelates. *Physical Review B*, 68(10), 104520.

**Citation:** Mervette El Batouti, et.al., (2019). "Preparation and Characterization of Unconventional Lanthanum Cerium Copuratethin Films Superconductors for Development of Thermoelectric Devices". *International Journal of Advanced Research in Chemical Science (IJARCS)*, 6(4), pp.46-56. DOI: <http://dx.doi.org/10.20431/2349-0403.0604004>.

**Copyright:** © 2019 Authors. This is an open-access article distributed under the terms of the Creative Commons Attribution License, which permits unrestricted use, distribution, and reproduction in any medium, provided the original author and source are credited.